

# Radiative Acceleration of Coronal Gas in Seyfert Nuclei

L. Binette

*European Southern Observatory, Casilla 19001, Santiago 19, Chile (E-mail: lbinette@eso.org)*

Accepted 18 December 1997. Received 27 August 1997

## ABSTRACT

The line ratios from coronal gas in Seyferts can be successfully fitted with photoionized clouds of high densities and low volume filling factor. The ionization parameter implied is sufficiently high that models must consider the effect of radiation pressure from the active nucleus. In spite of the nucleus gravitational force, radiation pressure is sufficiently strong to compress and radially accelerate the internally stratified gas clouds provided these contain small amounts of dust ( $\simeq 10\%$  of solar neighborhood value). This radial acceleration could explain the blueshift of the coronal lines relative to systemic velocity without the need of invoking an ambient ‘pushing’ wind. Embedded dust has the interesting effect of making the photoionized clouds marginally ionization bounded instead of matter bounded.

**Key words:** galaxies: Seyfert – galaxies: nuclei – line: formation

## 1 INTRODUCTION

Studies of the emission lines in Seyfert galaxies have indicated the presence of two different regions: a region of very high density with large velocity spread – the broad line region (BLR), and a region of low gas density with a much smaller velocity spread – the narrow line region (NLR). However, there is also a set of forbidden lines of extremely high excitation, the so-called ‘coronal’ lines which includes for instance [Fe VII]  $\lambda 6086$ , [Fe X]  $\lambda 6374$ , [S VIII]  $\lambda 9913$ , [Si VI]  $1.963\mu\text{m}$  and [Si VII]  $2.483\mu\text{m}$ . Most models favor photoionization over collisional ionization as excitation mechanism (e.g. Korista & Ferland 1989; Oliva et al. 1994; Moorwood et al. 1996). Earlier models considered that the filling factor of the coronal gas approached unity with a density lower than that of the NLR. The advent of far infrared measurements of the density sensitive [Ne V]  $14.3\mu\text{m}/24.3\mu\text{m}$  line ratio with ISO (Moorwood et al. 1996: Mo96), however, suggests much higher densities of  $\sim 5000\text{cm}^{-3}$  implying a very low volume filling factor for the coronal gas. In Paper I, Binette et al. (1997) proposed that these lines originate from individual gas clouds – as for the NLR – but characterized by an unusually high ionization parameter,  $U_0$  [cf. equation (1) below]. A similar gas geometry underlies the extensive grid of photoionization models of Ferguson, Korista & Ferland (1997). In Paper I, the clouds responsible for the coronal lines are always matter-bounded while they are essentially ionization-bounded in the models of Ferguson et al. (1997) or in the photoevaporating dusty cloud model of Pier & Voit (1995). One advantage of the matter-bounded clouds is that they are easier to accelerate by radiation pressure owing to their lower mass. Since the coronal lines are known to be

systematically blueshifted in Seyfert galaxies (Penston et al. 1984) relative to the systemic velocity (by  $35\text{km s}^{-1}$  in the case of Circinus, see Oliva et al. 1994; hereafter OSMM), our justification of using matter-bounded clouds was to account for this property by incorporating self-consistently the effect of radiation pressure in our cloud model.

The ionization parameters required to fit the very high excitation coronal lines is very high,  $U_0 \gtrsim 0.2$ , implying that the pressure exerted by the ionizing radiation exceeds the gas pressure (see Paper I). This has two interesting consequences: first, the photoionized cloud can be radially accelerated until the ram pressure it exerts on the ambient medium equals the pressure of the latter, this would account for the blueshift of the coronal lines for certain geometries, second, a density gradient arises within the clouds due to radiation pressure (a distributed force) and as shown in Paper I, the density stratification generated in this way leads to a wider range in excitation of the ionization species present in the cloud. The question addressed in this Letter is whether the pressure from the nuclear radiation field is sufficient to cause a strong radial acceleration of the clouds despite the gravitational pull exerted by the stars and the nuclear black hole.

## 2 THE MODEL

The multipurpose code MAPPINGS IC was used to compute the photoionization models. The atomic data is taken from a compilation of Ralph Sutherland (cf. Appendix in Ferruit et al. 1997). The uncertainties in collision strengths of many coronal lines are often large (see review by Oliva 1997 and

arXiv:astro-ph/9802244v1 18 Feb 1998

the discussion of the ‘iron conundrum’ by FKF) and may dominate the errors in the predicted line strengths.

### 2.1 Gas abundances and dust content $\mu_D$

As is customary and in the absence of other information, the abundances adopted will be solar (Anders & Grevesse 1989) but depleted according to the dust content. The latter is defined by the quantity  $\mu_D$  which is the dust-to-gas ratio of the plasma expressed in units of the solar neighborhood dust-to-gas ratio. The effects of dust on the thermal and ionization structure are taken into account (Binette et al. 1993). However, a different depletion scheme is defined whereby the destruction of dust grains is assumed to return uniformly the depleted elements (‘uniform return’). For instance, supposing  $\mu_D=0.1$  (i.e. 10% of the solar neighborhood dust content), the gas phase abundances are derived from the fully depleted set of abundances ( $\mu_D \equiv 1$ ) to which we reconstitute 90% of what has been depleted. This means that even for the heavily depleted elements like Ca, the gas phase abundance when  $\mu_D=0.1$  is 90% solar. The justification behind this is that small values of  $\mu_D$  are not the result of a different dust formation history but rather that of recent destruction (of normally formed dust) by sputtering, sublimation or optical erosion.

### 2.2 The ionizing continuum

We adopt a similar ionizing continuum as in Paper I, namely a powerlaw of index  $\gamma = -1.3$  ( $\varphi_\nu \propto \nu^{+\gamma}$ ) for the infrared-UV domain. This powerlaw joins at 2000 eV with a flatter powerlaw of index  $\gamma = -0.7$  to cover the X-ray domain. We impose a high energy cut-off of 100 keV (see Mathews & Ferland 1987). As is customary, we define the ionization parameter  $U_0$  as the ratio between the density of impinging ionizing photons and the gas density at the face of the cloud

$$U_0 = \frac{\int_{\nu_1}^{\infty} \varphi_\nu d\nu / h\nu}{cn_0} = \frac{q_0}{cn_0}, \quad (1)$$

where  $\varphi_\nu$  is the monochromatic energy flux impinging on the cloud,  $\nu_1$  the Lyman frequency,  $q_0$  the number of ionizing photons incident on the slab per  $\text{cm}^2$  per second,  $c$  the speed of light and  $n_0$  the total gas density at the irradiated surface of the slab (all quantities relevant to the irradiated surface carry 0 as a superscript or subscript).

### 2.3 Acceleration and pressure stratification

We adopt the formalism developed by Mathews (1986) and consider that our radially accelerated cloud has achieved internal hydrostatic equilibrium in the radial (outward) direction in the noninertial accelerating frame. Therefore, across a cloud (hereafter approximated as a slab) of total column density  $N_t$  and situated at a distance  $r$  from the black hole (BH), we have

$$\frac{1}{m_H} \frac{dP}{dN} = g_{rad}(N) - (g_{pull} + a_{cl}) = g_{rad}(N) - a', \quad (2)$$

where  $m_H$  is the proton mass,  $g_{rad}(N)$  the local radiative acceleration due to radiation pressure,  $g_{pull}$  the gravitational acceleration due to the central massive BH and the inner

stars, and  $a_{cl}$  the instantaneous acceleration of the entire cloud. The volume force exerted by radiation pressure is simply  $F_{rad} = nm_H g_{rad}(N)$  with its numerical expression in terms of photoelectric cross sections defined in Appendix A.3 of Paper I. The clouds geometrical thickness is considered negligible as compared to nuclear distance  $r$ , a good approximation in the current context of moderately thick clouds. This implies that for a cloud at  $r$ , the modified acceleration  $a'$  ( $= g_{pull} + a_{cl}$ ) is constant across its thickness  $N_t$ . We can regard  $a'$  as an eigenvalue for the acceleration of the cloud. In our scheme, the systematic shift\* towards the blue of the lines requires that  $a' > g_{pull}$ , that is  $a_{cl} > 0$  in equation (2). The blueshift can either be the result of an earlier acceleration of the clouds (the clouds have reached their terminal velocity against the opposing drag and gravitational forces), or of ongoing cloud acceleration.

### 2.4 Implementation in MAPPINGS IC

Independently of whether the acceleration corresponds to bulk motion or to inertial acceleration,  $a'$  is an important parameter for the cloud’s density structure. In our model, we express this input parameter in terms of the dimensionless quantity  $\Psi_0$  defined as  $\Psi_0 = a' / g_{rad}^0$  with  $g_{rad}^0$  the radiative acceleration at the irradiated face.

As described in Appendix of Paper I, MAPPINGS integrate equation (2) as well as simultaneously solve for the local ionization and thermal balance as a function of depth  $N$ . If  $U_0$  is sufficiently high, equation (2) implies a positive pressure gradient within the slab therefore leading to a strong density gradient across the photoionized slab. We define the relative pressure difference between the irradiated face and the back of the slab,  $\delta\Pi$ , as

$$\delta\Pi = (P_{gas}^{back} - P_{gas}^0) / \text{MIN}(P_{gas}^{back}, P_{gas}^0), \quad (3)$$

where the denominator represents the isotropic pressure,  $\widehat{P}$ , of the ambient cloud-confining medium. Note that  $\delta\Pi$  is approximately the ratio of dynamical pressure to ambient pressure. If  $\delta\Pi < 0$ , the cloud is experiencing a dynamical pressure at the inner irradiated surface (‘pushed’ clouds by an ambient wind), while if  $\delta\Pi > 0$  the clouds are suffering a drag force at their outer back surface as they are ‘pushing’ against the ambient medium. All the models presented below correspond to this latter case of  $\delta\Pi > 0$ .

For the dust-free matter bounded slab discussed in Paper I where we neglected inertial and bulk acceleration ( $\Psi_0 \equiv 0$ ), radiative pressure was shown to induce a pressure difference in the slab as high as  $\delta\Pi = 1.6$  when  $U_0=0.5$ . Since any realistic nuclear environment will imply a nonzero  $a'$  as a result of the gravitational field, it is the object of this study to investigate the effect of a positive  $\Psi_0$ .

In the general case of  $\Psi_0 > 0$ , because  $g_{rad}$  decreases monotonically with depth as the impinging radiation is gradually absorbed, the right term of equation (2) become negative at very large depths. This can result in  $\delta\Pi < 0$  depending on the choice of  $N_t$ ,  $\mu_D$  and  $\Psi_0$ . Although we could interpret this as being caused by ram pressure of an outflowing ambient medium (‘pushed’ cloud), this domain of

\* It is believed that we see one hemisphere only (i.e. one ionization cone) of the NLR in both Circinus and NGC 1068.

parameters has not been explored: first, because the aim of the Letter is to relate the line blueshift to the acceleration caused by radiation pressure and not to an extraneous alternative mechanism, second, because all the models considered below are not sufficiently thick to obtain  $\delta\Pi < 0$ .

To maximize the acceleration  $a'$ , it is useful to increase  $\Psi_0$  as much as possible. However, it was found that  $\Psi_0=0.5$  which is adopted hereafter cannot be exceeded significantly (otherwise  $\delta\Pi$  shrinks considerably). In effect,  $\Psi_0=0.5$  maintains two essential effects: it still allows a significant density gradient (therefore optimizing the line ratio fit, cf. Paper I) and it results at the same time in a strong acceleration  $a'$ . Clouds submitted to significant radiation pressure are particularly prone to derimming through the establishment of a lateral flow as shown by Mathews (1986). For a review of the problem of cloud stability under conditions appropriate to the NLR, see Mathews & Veilleux (1989).

### 3 THE EXCITATION OF THE CORONAL GAS IN CIRCINUS AND NGC 1068

All detailed studies of the coronal gas reveal that the emitting gas encompasses many stages of excitation. This indicates that this gas must be significantly thick to the ionizing radiation rather than very optically thin. We can envisage two geometries, one broadly spherical and filled with low density gas: the onion ring geometry (Korista & Ferland 1989; OSMM) the other consists of an ensemble of clouds of very low filling factor and therefore similar to the NLR gas in general except for its much higher excitation. What is clear is that although the range of ionization species of the coronal gas is wide, it does not encompass the very low excitation species of [O II], [O I], [S II]... since the latter appear to be kinematically distinct as shown by OSMM and Marconi et al. (1996). In Paper I, this was interpreted as an indication that the coronal line emitting clouds were matter bounded as was also thought to be the case for the high excitation clouds of the ENLR and NLR (?; Wilson et al. 1997).

The thickness of the clouds is not defined arbitrarily but can be empirically set by the ratio between the highest and the lowest excitation species belonging to the coronal gas. In Paper I it was found that the lines of [Si VI] 1.963 $\mu\text{m}$  and [Si IX] 3.935 $\mu\text{m}$  worked very well for this purpose. The same procedure is adopted here whereby the slab is truncated at the point where the modeled [Si VI]/[Si IX] ratio matches the observed value. It is interesting to note that in the *dust-free* case, despite the difference in excitation between the two Seyferts, this truncation always seems to occur after  $\sim 60$ –65% of the ionizing photons have been *absorbed*.

#### (i) The Circinus galaxy.

If we repeat the dust-free calculations of Paper I with  $U_0=0.5$  and density  $n_0=1200\text{ cm}^{-3}$  but set  $\Psi_0=0.5$ , we find that the modified acceleration is only  $a' = 2.9 \times 10^{-7}\text{ cm s}^{-2}$  (i.e.  $g_{rad}^0$  is twice that value). As shown later in Section 4.1, this is at least an order of magnitude below the acceleration due to the gravity exerted by the stars within 100 pc of the nucleus of the Milky Way. It would therefore appear that radiation pressure is insufficient in accelerating radially the line emitting gas. However, if we allow trace quantities of dust to be present in the cloud, radiation pressure is much

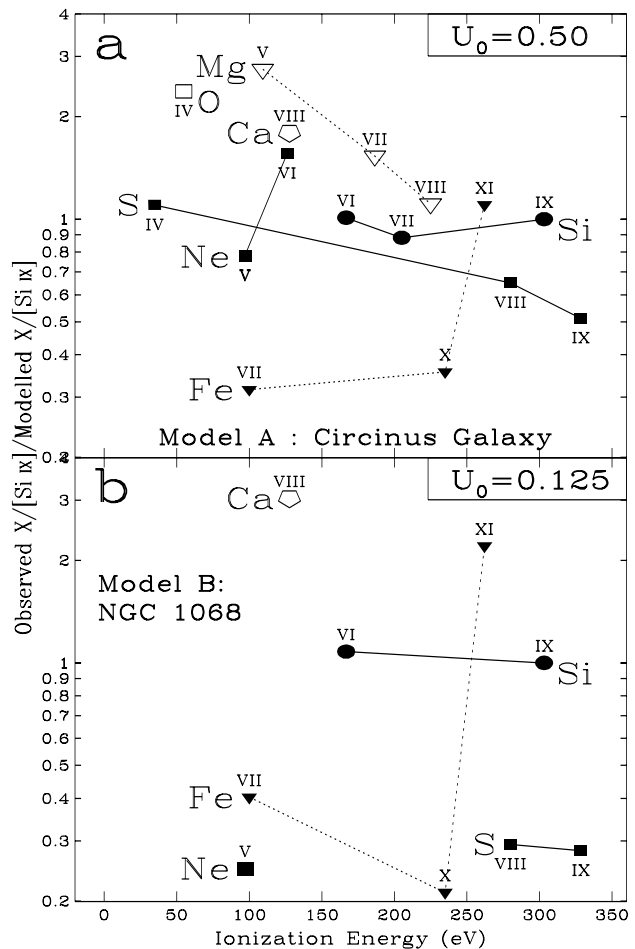


**Figure 1.** Observed divided by modeled line flux ratios for (a) the Circinus galaxy and (b) NGC 1068. All ratios are expressed relative to [Si IX] 3.935 $\mu\text{m}$ . Both models A and B have  $n_0=1200\text{ cm}^{-3}$  and a dust content of 10% of the solar neighborhood dust-to-gas ratio ( $\mu_D=0.1$ , see text and Table. 1). The lines plotted in (a) include [O IV] 25.90 $\mu\text{m}$ , [Si VI] 1.963 $\mu\text{m}$ , [Si VII] 2.483 $\mu\text{m}$ , [Si IX] 3.935 $\mu\text{m}$ , [S IV] 10.54 $\mu\text{m}$ , [S VIII]  $\lambda 9913$ , [Ca VIII] 2.32 $\mu\text{m}$ , [Si X] 1.25 $\mu\text{m}$ , [Ne V] 14.32 $\mu\text{m}$ , [Ne VI] 24.31 $\mu\text{m}$ , [Ne VI] 7.66 $\mu\text{m}$ , [Fe VII]  $\lambda 6086$ , [Fe X]  $\lambda 6374$ , [Fe XI]  $\lambda 7892$ , [Mg V] 5.62 $\mu\text{m}$ , [Mg VII] 5.51 $\mu\text{m}$  and [Mg VIII] 3.03 $\mu\text{m}$ .

higher and dust absorption even dominates the photoelectric absorption terms contained in  $g_{rad}$ . For instance, if we set  $\mu_D=0.1$ , we obtain  $a' = 2.6 \times 10^{-6}\text{ cm s}^{-2}$ . The modeling of the observed line ratios reported by Mo96 and OSMM is presented in Fig. 1a (Model A) using  $\mu_D=0.1$ . The fit is of comparable quality to that presented in Paper I or in Mo96. As can be expected, the effect of ‘uniform return’ depletion on the [Ca VIII] point is less than 0.05 dex (see Section 2.1). The resultant pressure stratification is somewhat smaller at  $\delta\Pi=1.2$ . It was found that arbitrarily increasing either  $\mu_D$  or  $\Psi_0$  to higher values degraded significantly the fit to the Circinus line ratios.

The hypothesis of internal dust is also present in the comprehensive dusty cloud model of Pier & Voit (1995). In their

model, the strong radiation pressure exerted on the dusty gas (situated near the inner molecular torus) leads to progressive cloud evaporation and to the creation of an X-ray-heated wind. The smaller dust content and cloud's thickness of the matter-bounded clouds presented in this Letter leads to a smaller extinction ( $A_V \simeq 0.15$ ) than in Pier & Voit (1995).

(ii) The Seyfert galaxy NGC 1068.

We follow a similar procedure in the case of NGC 1068. The observational data is taken from Marconi et al. (1996). The set of lines is not as complete but is probably sufficient for estimating  $U_0$ . Marconi et al. reported that the excitation was lower than in Circinus. A similar result is found here. A value four times lower than in Circinus leads to a reasonable fit to the gas *excitation* as revealed by the S and Si line ratios. The fit is shown in Fig. 1b (Model B:  $U_0=0.125$  and  $\mu_D=0.1$ ). Systematic but equal departures from unity (e.g. the S lines) might partly be due to peculiar abundances relative to solar. In this model, we arbitrarily adopted the same density as for Circinus since no published measurements of the density from the [Ne v]  $14.3 \mu\text{m}/24.3 \mu\text{m}$  ratio was available at the time of writing. The excitation indicated by the ratio [Fe VII]/[Fe X] is not so badly fitted but [Fe XI]  $\lambda 7892$  is certainly discrepant. As was the case for Circinus, assigning more than 50% of the radiation pressure to cloud acceleration (i.e.  $\Psi_0 > 0.5$ ) was found to worsen the fit. On the other hand, the amount of dust allowed did not appear to strongly affect the fit as long as  $\mu_D \leq 0.5$ . A good fit to the value of  $a'$  as a function of the dust content is  $a' = (n_0/1200)(U_0/0.125) [3.1 \times 10^{-7} + 5.8 \times 10^{-6} \mu_D]$ .

If we vary  $n_0$  and keep the ionization parameter constant, by equation (1)  $q_0$  must scale with  $n_0$ . Therefore the modified accelerations  $a'$  will also scale linearly with  $n_0$  since radiation pressure scales with ionizing flux. Note that a similar model to that of Fig. 1b but for which the dust content has been increased to  $\mu_D=0.3$  (i.e. Model C in Table 1), the acceleration  $a'$  becomes comparable to that of Model A with  $U_0$  four times larger (but three times less dust).

For Models A and B, the contrast between the density at the irradiated face and the 'emissivity averaged' value,  $\bar{n}/n_0$ , is 3.75 and 1.75 respectively. Table 1 list other relevant quantities for the two models shown in Fig. 1 as well as for a dustier Model C characterized by  $\mu_D=0.3$ .

## 4 RESULTS

For an empirically determined value of  $U_0$ ,  $a'$  will scale linearly with the ionizing flux  $q_0$ . Therefore, for a given value of  $U_0$ , the predicted value of  $a'$  scales linearly with the assumed value of the density  $n_0$ . Using the [Ne v]  $14.3 \mu\text{m}/24.3 \mu\text{m}$  line ratio, one can determine the density of the coronal line region and therefore  $a'$ . It is found that the mean density  $n_0$  as defined in Paper I for a pressure stratified slab is the same as that inferred from the calculated far-infrared [Ne v] line ratio. Therefore this line ratio reveals us the 'characteristic' density of the highly excited component. Having determined empirically the ionization parameter characterizing the coronal gas in two AGN, we can now proceed to compare the calculated  $a'$  of models with,  $g_{pull}$ , the strength of the gravitational field expected in a galactic nucleus.

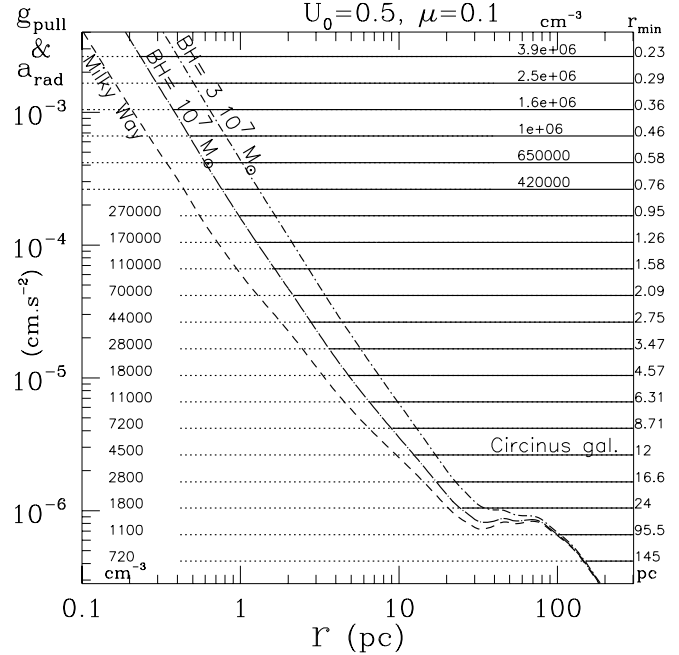


**Figure 2.** A plot of the gravitational pull,  $g_{pull}$ , exerted by the nuclear mass distribution of the Milky Way (dash line) as a function of galactic radius. The continuous and the dash-dotted lines consider the effect of a more massive BH of  $10^7$  or  $3 \times 10^7 M_\odot$ , respectively (see Section 4.1). The modified acceleration  $a'$  due to radiation pressure for clouds of different densities  $\bar{n}$  is indicated using horizontal lines (whatever  $\bar{n}$ , it is assumed that  $U_0=0.5$ ). The minimum radius for which coronal gas emission can be accelerated (i.e.  $a' \geq g_{pull}$ ) is indicated in the right margin for the case of a  $10^7 M_\odot$  BH.

### 4.1 The nuclear mass model: $M_{*+bh}(r)$

For radiative acceleration to be responsible of the blueshift of the coronal lines, it must overcome the gravitational pull of the combined mass of the central stars and the nuclear BH. To illustrate the force entailed, let us adopt the better studied Milky Way mass distribution,  $M_{*+bh}(r)$ , inside a radius  $r \leq 200$  pc. From 0.1 to 2 pc we borrow the mass model of Genzel et al. (1997) which we join at 2 pc to the isotropic orbit stellar mass model of Lindqvist et al. (1992; cf. their Table 3) which is based on the projected mass method for a dominant central mass. The resultant gravitational pull is simply  $g_{pull} = GM_{*+bh}/r^2$  and is plotted in Fig. 2 (dash line). One interpretation proposed by Genzel et al. for the innermost mass is that it might consist of a BH of  $\approx 2.8 \times 10^6 M_\odot$ . Note that beyond  $r \gtrsim 30$  pc the gravitational pull from the stars dominate that of the BH. On account of the much stronger nuclear activity characterizing Seyferts, it is plausible that a typical AGN could have a more massive BH than the Milky Way. For instance, estimates of the central mass in NGC 1068 ranges from  $10^7 M_\odot$  (Greenhill & Gwinn 1997) to  $3 \times 10^7 M_\odot$  (Gallimore et al. 1996). In an attempt to allow for this possibility, the effect of simply substituting a more massive point source is shown in Fig. 2 in which the continuous and the dotted-dash curves correspond to BH masses of  $10^7 M_\odot$  and  $4 \times 10^7 M_\odot$ , respectively.

**Table 1.** Parameters characterizing the models.

Model	$U_0$	$n_0$	$\mu_D$	$N_t/10^{21}$	$\bar{n}$	$A_V$	$\delta\Pi$	$a'/10^{-6}$	$\bar{n}/n_0$	$q_{back}/q_0^a$	$g_{dyn}/g_{rad}^b$	$\widehat{P}/k/10^7 K^c$	L (pc) <sup>d</sup>
A	0.50	1200	0.10	6.2	4500	0.15	1.22	2.63	3.75	0.06	-0.36	13.2	0.68
B	0.125	1200	0.10	3.0	2100	0.07	0.51	0.89	1.75	0.22	-0.46	7.8	0.55
C	0.125	1200	0.30	2.6	2000	0.19	0.25	2.05	1.65	0.04	-0.18	8.1	0.35

<sup>a</sup> Fraction of ionizing photons escaping the slab unabsorbed.

<sup>b</sup> Ratio of dynamical acceleration to total radiative acceleration (Mathews 1986).

<sup>c</sup> Isotropic pressure of the ambient cloud-confining medium. It would scale with  $n_0$  if  $U_0$  is kept constant.

<sup>d</sup> Geometrical depth of the slab in parsecs. L would scale inversely with  $n_0$  if  $U_0$  is kept constant.

## 4.2 Minimum NLR radius

It is not possible at this point to realistically assess how different the nuclear stellar field would be in either more massive galaxies than ours or in nuclei with more massive BHs. With this caveat in mind, let us adopt the continuous curve in Fig. 2 of a  $10^7 M_\odot$  BH as being representative of low luminosity AGN. After determining the different values of  $a'$  expected if we simply vary  $n_0$  of Model A (with  $U_0=0.5$ ), we can proceed to derive the minimal radius beyond which the clouds have their acceleration  $a'$  exceed  $g_{pull}$ . The allowed domain in  $r$  for uniform acceleration of the coronal gas lies to the left of the  $g_{pull}$  curve in Fig. 2 as shown by the horizontal *solid* lines, each corresponding to different values of the mean densities  $\bar{n}$ . For the particular case of the Circinus galaxy for which we know the density, a minimum radius of 12 pc is inferred inside of which the coronal gas would fall or stall instead of being radially accelerated. The true position of the nucleus in Circinus is not known with precision since its nucleus is heavily reddened and the true kinematic centre may not correspond to the continuum peak. We cannot yet therefore verify the validity of  $r_{min}$ . However, in the case of NGC 1068, Marconi et al. (1996) found that the infrared lines were displaced by  $0.5''$  from the optical continuum peak, which corresponds to a nuclear offset of  $\simeq 40$  pc ( $D=18$  Mpc). The gas density is not yet determined but if comparable to Circinus, we would expect a much larger  $r_{min}$  in NGC 1068 based on its lower excitation by a factor four.

The main conclusions are the following. Provided there is dust left out in the gas, radiation pressure not only can induce a density gradient in the photoionized clouds but also be responsible for their outward acceleration despite the presence of strong gravitational field. It is found that higher values than  $\mu_D=0.1$  are detrimental to the fit in the case of Circinus. Based on empirically measured densities and excitation, a minimum nuclear distance  $r_{min}$  is predicted to characterize the *observable* coronal gas. The higher the density, the smaller  $r_{min}$ . The advent of high spatial resolution line mapping will allow testing whether such a correspondence between  $r$  and  $\bar{n}$  exists. Finally, because of the large value of  $U_0$ , the fraction of ionizing photons escaping the clouds can be quite small even with small amounts of dust. By empirically setting the thickness of the clouds to be such that the observed [Si VI]/[Si IX] ratio is reproduced by the model, one finds that only 6% of the impinging photons in Model A are *not* absorbed (instead of 35–40% in the dust-free case). One may therefore conceive the possibility that the coronal clouds are not matter bounded but marginally thick and bounded by dust absorption. The most inner nuclear regions (presumably of higher visibility in Seyferts 1)

which still emit coronal lines may correspond to the missing domain between the BLR and the NLR (this gas would have to be proportionally denser to have  $a' \geq g_{pull}$ ). In effect, as shown by Netzer & Laor (1993), dust embedded photoionized gas of high excitation presents a greatly reduced line efficiency explaining the relative line weakness of this putative intermediate region.

## REFERENCES

- Anders E., Grevesse N., 1989, *Geochim. Cosmochim. Acta*, 53, 197
- Binette L., Wang J., Villar-Martin M., Martin P. G., Magris G., 1993, *ApJ*, 414, 535
- Binette L., Wilson A. S., Raga A., Storchi-Bergmann T., 1997, *A&A*, 327, 909
- Ferguson J. W., Korista K. T., Ferland G. J., 1997, *ApJS*, 110, 287 (FKF)
- Ferruit P., Binette L., Sutherland R. S., Pécontal E., 1997, *A&A*, 322, 73
- Gallimore J. F., Baum S. A., O'Dea C. P., Brinks E., Pedlar A., *ApJ*, 462, 740
- Genzel R., Thatte N., Krabbe A., Kroher H., Tacconi-Garman L. E., 1997, *ApJ*, in press (MPE preprint #362)
- Greenhill L. J., Gwinn C. R., 1998, in *proc. of the NGC 1068 Workshop*, AP&SS, 249, 261
- Korista K. T., Ferland G. J., 1989, *ApJ*, 343, 678
- Lindqvist M., Habing H. J., Winnberg A., 1992, *A&A*, 259, 118
- Marconi A., van der Werf P. P., Moorwood A. F. M., Oliva E., 1996, *A&A*, 315, 335
- Mathews W. G., 1986, *ApJ*, 305, 187
- Mathews W. G., Ferland G. J., 1987, *ApJ*, 323, 456
- Mathews W. G., Veilleux S., 1989, *ApJ*, 336, 93
- Moorwood A. F. M., Lutz D., Oliva E., Marconi A., Netzer H., Genzel R., Sturm E., de Graauw T., 1996, *A&A*, 315, L109 (Mo96)
- Netzer H., Laor A., 1993, *ApJ*, 404, L51
- Oliva E., 1997, in Peterson, B. M., Cheng, F.-Z., Wilson, A. S., ed., *ASP Conf. Ser. Vol. 113, Emission lines in active galactic nuclei: new methods and techniques*, Astron. Soc. Pac., San Francisco, p. 288
- Oliva E., Salvati M., Moorwood A. F. M., Marconi A., 1994, *A&A*, 288, 457 (OSMM)
- Penston M. V., Fosbury R. A. E., Bokserberg A., Ward, M. J., Wilson A. S., 1984, *MNRAS*, 208, 347
- Pier E. A., Voit G. M., 1995, *ApJ*, 450, 628
- Wilson A. S., Binette L., Storchi-Bergmann T., 1997, *ApJ*, 482, L131

This paper has been produced using the Royal Astronomical Society/Blackwell Science L<sup>A</sup>T<sub>E</sub>X style file.